

Extended Bose Hubbard model of interacting bosonic atoms in optical lattices: from superfluidity to density waves

G. Mazzarella, S. M. Giampaolo, and F. Illuminati

Dipartimento di Fisica “E. R. Caianiello”, Università di Salerno,

Coherentia CNR-INFM, and INFN Sezione di Napoli,

Gruppo Collegato di Salerno, Via S. Allende, 84081 Baronissi (SA), Italy

(Dated: November 16, 2005)

For systems of interacting, ultracold spin-zero neutral bosonic atoms, harmonically trapped and subject to an optical lattice potential, we derive an Extended Bose Hubbard (EBH) model by developing a systematic expansion for the Hamiltonian of the system in powers of the lattice parameters and of a scale parameter, the *lattice attenuation factor*. We identify the dominant terms that need to be retained in realistic experimental conditions, up to nearest-neighbor interactions and nearest-neighbor hoppings conditioned by the on site occupation numbers. In mean field approximation, we determine the free energy of the system and study the phase diagram both at zero and at finite temperature. At variance with the standard on site Bose Hubbard model, the zero temperature phase diagram of the EBH model possesses a dual structure in the Mott insulating regime. Namely, for specific ranges of the lattice parameters, a density wave phase characterizes the system at integer fillings, with domains of alternating mean occupation numbers that are the atomic counterparts of the domains of staggered magnetizations in an antiferromagnetic phase. We show as well that in the EBH model, a zero-temperature quantum phase transition to pair superfluidity is in principle possible, but completely suppressed at lowest order in the lattice attenuation factor. Finally, we determine the possible occurrence of the different phases as a function of the experimentally controllable lattice parameters.

I. INTRODUCTION

In the last years we have witnessed a spectacular acceleration in the experimental manipulation of neutral atoms in optical lattices [1, 2, 3, 4] that has opened the way to the simulation of quantum complex systems of condensed matter physics, such as high- T_C superconductors, Hall systems, and superfluid 4He , thanks to the extreme flexibility and controllability of such atom-optical systems [5]. Optical lattices are stable periodic arrays of microscopic potentials created by the interference patterns of intersecting laser beams [6]. Atoms can then be confined in different lattice sites, and by varying the strength of the periodic potential it is possible to tune the interatomic interactions with great precision and to enhance them well into the regime of strong correlations, even in the dilute limit. The transition to a strong coupling regime can be realized by increasing the depth of the lattice potential wells, a quantity that is directly proportional to the intensity of the laser light which, in turn, is an experimental parameter that can be controlled with great accuracy. For this reason, besides the fundamental interest for the investigation of quantum phase transitions [7, 8, 9, 10] and other collective quantum phenomena [11, 12, 13, 14, 15, 16], optical lattices have become an important tool in applications ranging from laser cooling [17] to quantum control and information processing [18, 19], and quantum computation [20, 21, 22, 23, 24].

The theory of neutral bosonic atoms in optical lattices has been originally developed, in its simplest framework, by assuming that the atoms are confined to the lowest Bloch band of the periodic optical potential [25, 26]. It is then straightforward to show that in this approximation

the system is very well described by the standard, on site Bose Hubbard model. In such a model a superfluid-Mott insulator (SF-MI) transition is predicted to occur when the energy gap between the local ground state and the first excited levels becomes comparable to the hopping energy between adjacent lattice sites [7, 8, 9, 10]. Moreover, no major qualitative changes appear when higher excited energy levels of the external trapping potentials are considered [27]. This prototypical quantum phase transition can be realized experimentally, for instance by manipulating the strength of the lattice potential, which results in a controlled change of the kinetic (hopping) energy term [5]. Following this kind of approach, the superfluid-Mott insulator quantum phase transition has been realized in a series of beautiful experiments, by loading an ultracold atomic Bose-Einstein condensate in a three-dimensional optical lattice [4]. At finite temperature and in the strong coupling regime, the quantum phase transition is smeared in a classical transition from a completely disordered regime to an ordered, superfluid phase (SF) [10, 27]. Finally, if more complicated geometrical settings such as optical superlattices, networks, and graphs, are considered, interesting unconventional interplays between the different quantum phases may appear [28, 29, 30, 31, 32].

In the on site Bose Hubbard (BH) model all the terms deriving from two-body interactions between the bosonic atoms are neglected except the local ones taking place on a same site of the optical lattice. This is often an excellent approximation. However, microscopic interactions are in general of finite range, and it may be interesting to address the problem of the physical picture that emerges if one takes into account two-body inter-

actions between sites at non-vanishing distance and/or hopping amplitudes beyond nearest-neighbor sites. This problem has been extensively studied in the case of charged fermions, which are endowed with very long range Coulomb interactions, usually by introducing extended Fermi Hubbard models with nearest-neighbor interaction terms [33, 34, 35, 36, 37]. Extended Fermi Hubbard models are prototypical in theoretical condensed matter physics, because they are believed to be more realistic approximations to the true inter-electronic interactions and moreover exhibit richer phase diagrams when compared to the standard Hubbard model, especially in low spatial dimensions [38, 39, 40].

In the present paper, we extend this kind of analysis to the bosonic case, and we introduce and study a type of extended Bose Hubbard model for the description of interacting bosons in regular lattices. Our study, although general, will be mainly concerned with the analysis of realistic physical systems such as dilute ensembles of interacting spin-zero bosonic neutral atoms subject to an optical lattice potential and spatially confined by a slowly varying harmonic trapping. Confining our attention to the lowest band of the optical lattice potential, we construct an effective extended Bose Hubbard Hamiltonian, that emerges when we take into account the terms deriving from the boson-boson interactions both on the same lattice site and on pairs of nearest neighbors. Our aim is then to analyze the phase transitions that may occur in such systems both at zero and at finite temperature, and determine the general features of the associated phase diagrams.

The paper is organized as follows: In Sec.II we set the general notations, the needed tools, and derive the model Hamiltonian from the underlying microscopic dynamics in second quantization. We identify an exponential lattice scale factor, the *lattice attenuation factor* that gives rise to a natural expansion parameter for the Hamiltonian of the system. In this way we are able to determine all the dominant terms that need to be retained in a power series expansion of the different energy contributions, that add to the terms of the standard Bose Hubbard (BH) model Hamiltonian. These additional terms can be easily identified and ordered in increasing powers of the lattice attenuation factor and include nearest-neighbor interactions, nearest-neighbor hoppings of single atoms conditioned by the on site occupation number, and nearest-neighbor hoppings of atomic pairs (bosonic pairs). The ensuing Hamiltonian defines a type of extended Bose Hubbard (EBH) model of interacting bosons in the lowest Bloch band. Other types of EBH models can be obtained by considering interactions with far neighbors, and can be related to the fractional quantum Hall effect [41]. Other different types of Hubbard-like models can also be obtained, at least for one-dimensional fermionic systems, by implementing appropriate mode expansions of the second-quantized fermionic field operators, as recently shown by Massel and Penna [42].

Our treatment assures the explicit dependence on the

physical parameters of realistic optical lattice potentials and external confining harmonic potentials, does not involve issues of metastability and lifetime for states living in excited bands, allows the study of the phase diagram both at zero and at finite temperature, and is based on a systematic expansion that connects any EBH model to the underlying microscopic dynamics in second quantization. Finally, it can be in principle extended to more general situations, including multi-species bosonic systems and Fermi-Bose mixtures of bosonic and fermionic atoms. Other generalizations of the on site Hubbard model are of course possible by including Bloch bands of higher order in the description. Two such possible EBH models with inter-band hoppings and interactions have been recently proposed in connection with schemes to generate metastable excited states of cold atoms in optical lattices [43, 44].

In Sec.III, we analyze the phase diagram of the extended Bose Hubbard model (EBH) in the standard grand canonical formalism. We first consider the structure of the quantum phases at zero temperature, when all the kinetic terms vanish (strong coupling regime). Remarkably, in this case the model is mapped into a quantum antiferromagnetic Ising model in the presence of an external magnetic field. As it is well known, this model undergoes a quantum transition between a ferromagnetic and an antiferromagnetic phase [45]. As a consequence, in a small range of parameters (very strong coupling regime) for a system of bosons in an optical lattice, there exists a new insulator phase in which the atomic density is not constant on each lattice site. This new quantum phase can be seen as a Density Wave Mott Insulator (DWMI), and is of course absent in the on site BH model that can sustain only a Pure Mott Insulator (PMI) phase at constant density. In the DWMI phase, there appear two alternating domains (sublattices) of different mean on site occupation numbers, that are the atomic counterparts of the domains of different staggered magnetization in the antiferromagnetic phase of the quantum Ising model. Next, we reintroduce the kinetic terms in the EBH Hamiltonian by resorting to Bogoliubov-like and mean field approximations. In this framework three real-valued order parameters emerge: the conventional single boson (single atom) superfluid order parameter, a new bosonic pair superfluid order parameter, and finally the mean number of bosons (atoms) per site. These parameters are not all independent from each other, due to the existence of physical constraints on thermodynamic stability and on the PMI-DWMI phase separation.

In Sec.IV, we present qualitative and analytical studies of the different possible phases in the presence of non vanishing kinetic energy terms. In this case, minimization of the free energy with respect to the different order parameters yields that the only superfluid transition which can occur is the one ruled by the single atom SF order parameter. We analyze the behavior of the SF-PMI and the SF-DWMI quantum phase transitions at zero temperature, and the behavior of the SF single boson order parameter

at finite temperature. We study the critical temperature of the disordered-SF phase transition as a function of the filling factor and of the lattice depth. Then, starting from finite temperatures, we analyze the possibility to recover the SF-PMI and the SF-DWMI quantum phase transitions by determining the behavior of the critical energy gap in the limit of vanishing temperature, as a function of the lattice depth and for different values of the trapping frequencies. Finally, in Sec.V we give some concluding comments on the obtained results and discuss some possible directions for future research.

II. GENERAL SETTING

The microscopic Hamiltonian for an ensemble of bosonic atoms that are confined by a slowly varying external harmonic trapping potential and subject to an additional optical lattice can be written as

$$\hat{H} = \hat{T} + \hat{V} + \hat{W}, \quad (1)$$

where \hat{T} is the kinetic energy term that reads

$$\hat{T} = -\frac{\hbar^2}{2m} \int d\vec{r} \hat{\Psi}^\dagger(\vec{r}) \nabla^2 \hat{\Psi}(\vec{r}), \quad (2)$$

with $\hat{\Psi}(\vec{r})$ being the bosonic annihilation field operator at point \vec{r} . On the other hand \hat{V} represents the contribution of the external potential to the energy:

$$\hat{V} = \int d\vec{r} \hat{\Psi}^\dagger(\vec{r}) (V_H(\vec{r}) + V_{opt}(\vec{r})) \hat{\Psi}(\vec{r}). \quad (3)$$

In concrete situations, spatial confinement of the atoms is provided by the quadrupolar anisotropic trapping magnetic field that leads to an harmonic trapping potential of the form

$$V_H = \frac{m\omega^2}{2} (x^2 + \lambda^2 y^2 + \lambda^2 z^2), \quad (4)$$

where ω is the frequency associated to the harmonic trap in the x direction and λ is the anisotropic coefficient, i.e. the ratio between the frequency in the yz plane and the frequency in the x direction. The most common experimental settings are realized in the so-called “cigar-shaped” configuration ($\lambda \gg 1$). Correspondingly, the second contribution to the potential energy is a 1-D periodic potential needed to realize the optical lattice along the axis of the “cigar”:

$$V_{opt}(x) = V_0 \sin^2\left(\frac{\pi x}{a}\right), \quad (5)$$

where V_0 is the maximum amplitude of the light shift associated to the intensity of the laser beam and a is the lattice spacing related to the wave vector k of the standing laser light by $k = \pi/a$.

Finally, the third contribution is the local, contact two-body interaction

$$\hat{W} = \frac{g_{BB}}{2} \int d\vec{r} \hat{\Psi}^\dagger(\vec{r}) \hat{\Psi}^\dagger(\vec{r}) \hat{\Psi}(\vec{r}) \hat{\Psi}(\vec{r}), \quad (6)$$

in which the interaction coupling $g_{BB} = 4\pi\hbar^2 a_{BB}/m$ where m is the atomic mass and a_{BB} is the atom-atom (boson-boson) s -wave scattering length. In the following, we will always assume boson-boson repulsion, i.e. $a_{BB} > 0$.

In the presence of a strong optical lattice and a sufficiently shallow external confinement in the x direction, so that at any lattice site its value can be considered constant, the bosonic field operators can be expanded in the basis of the single-particle Wannier wave-functions localized at each lattice site x_i . Since the typical interaction energies involved are normally not strong enough in order to excite higher vibrational states, we can retain only the the lowest vibrational state in each lattice potential well (single-band approximation). In the case of stronger external confinements, or interactions, one should include higher Bloch bands as well in the expansion of field operators, a case we do not consider in the present context. Moreover, as far as the harmonic trapping potential is concerned, we have shown in a previous work [27] that the introduction of higher energy levels of the harmonic oscillator does not modify the basic phenomenology of the system. Under these conditions, we can avoid working directly with the exact Wannier wave functions and replace them, with an excellent degree of fidelity, with their harmonic-oscillator approximations at each optical lattice well. Then, the Wannier wave functions $w(\vec{r})$ factorize in the product of harmonic oscillator states in each direction:

$$\hat{\Psi}(\vec{r}) = \sum_i \hat{a}_i w(x - x_i) w(y) w(z), \quad (7)$$

where x_i is the center of the i -th lattice well and \hat{a}_i is the bosonic annihilation operator acting at the i -th lattice site. In each lattice potential well, the Wannier local ground states are Gaussians in the harmonic approximation:

$$\begin{aligned} w(x - x_i) &= \frac{1}{\sqrt{l_x \sqrt{\pi}}} \exp\left[\frac{-(x - x_i)^2}{2l_x^2}\right], \\ w(y) &= \frac{1}{\sqrt{L_\perp \sqrt{\pi}}} \exp\left[\frac{-y^2}{2L_\perp^2}\right], \\ w(z) &= \frac{1}{\sqrt{L_\perp \sqrt{\pi}}} \exp\left[\frac{-z^2}{2L_\perp^2}\right]. \end{aligned} \quad (8)$$

In Eq. (8) we have introduced the harmonic oscillator lengths of the ground state in the y and z directions $L_\perp = \sqrt{\hbar/(m\lambda\omega)}$, and the oscillator length in the harmonic approximations of the periodic potential l_x that reads, as a function of the lattice parameters, $l_x = (a^4 E_R / (\pi^4 V_0))^{1/4}$, where $E_R = (\pi\hbar)^2 / 2a^2 m$ is the

lattice recoil energy. In this paper we will consider the physical situation of very shallow trapping potentials, such that $L_x \equiv L_\perp \sqrt{\lambda} \gg aM$, with M denoting the total number of lattice sites. As a consequence, the local density approximation (LDA) can be applied. Therefore, when exploiting the expansion Eq. (7) to map the full microscopic Hamiltonian Eq. (1) into its lattice version, we will discard all terms that are of order $(aM/L_x)^2$ or higher. Qualitatively, this means neglecting those nonlocal effects that are induced by the presence of the trapping potentials, such as site-dependent hopping terms. The latter can become important in regions of the lattice very far out of the central core of the harmonic trap. However, the typical experimental situations involve only that part of the lattice that lies well inside the central core of the slowly varying confining potential [46]. We can then write down the translationally invariant lattice version of Hamiltonian Eq. (1) in the form

$$\hat{H} = -\frac{1}{2} \sum_{i,j} t_{i,j} \hat{a}_i^\dagger \hat{a}_j + \frac{1}{2} \sum_{i,j,k,l} U_{i,j,k,l} \hat{a}_i^\dagger \hat{a}_j^\dagger \hat{a}_k \hat{a}_l . \quad (9)$$

In Eq. (9) $U_{i,j,k,l}$ is the two-body interaction strength that involves four sites of the lattice that depends on the relative distance between the sites involved. Recalling the expression of the two-body interaction Eq. (6), together with the form of the bosonic field operator Eq. (7) and of the lattice wave functions Eq. (8), one has

$$U_{i,j,k,l} = U_0 \varepsilon^{\gamma/2} , \quad (10)$$

where

$$U_0 = (2\pi)^{-\frac{3}{2}} \frac{g_{BB}}{l_x L_\perp^2} , \quad (11)$$

is the local interaction strength, i.e. the amplitude of the interaction when $i = j = k = l$,

$$\varepsilon = \exp(-a^2/4l_x^2) , \quad (12)$$

is the *lattice attenuation factor*, and

$$\begin{aligned} \gamma = & (i-j)^2 + (i-k)^2 + (i-l)^2 \\ & + (j-k)^2 + (j-l)^2 + (k-l)^2 , \end{aligned} \quad (13)$$

is the “four-site distance” relative to all possible independent pairs of sites that can be chosen out of a set of four sites. It is worth noticing that ε can be re-expressed in the form $\varepsilon = \exp(-\pi^2 \sqrt{s}/4)$, i.e. in terms of an experimentally measurable and tunable quantity, the depth s of the lattice wells: $s = V_0/E_R$.

On the other hand, in Eq. (9), $t_{i,j}$ is the strength of the contributions of the kinetic and the external potential terms to the energy. For $i = j$ it gives rise to a constant zero point energy term that can be discarded by redefining the zero of the energy; if $i \neq j$ it represents the probability amplitude for an atom to tunnel from the i -th lattice site to the j -th one along the x direction. Obviously, also this probability amplitude is a function of the distance between the involved sites, but it is impossible to write for it a closed analytical formula like Eq. (10). However, from the form of Eq. (8) it is easy to show that $t_{i,j}$ is still proportional to some positive power of the lattice attenuation factor ε , with the exponent depending only on the distance between the sites. Hence, in general one can write

$$t_{i,j} = J_{|i-j|} \varepsilon^{(i-j)^2} , \quad (14)$$

where $J_{|i-j|}$ decreases as a polynomial function of the modulus of the distance between the sites. Taking into account the form of the kinetic energy Eq. (2), the forms of the external potentials Eq. (3), Eq. (4), and Eq. (5), together with the expression of the bosonic field operators Eq. (7) and of the lattice wave functions Eq. (8), for $|i-j| = 1$ (nearest neighbors) one has

$$J_1 = V_0 \left(\frac{\pi^2}{2} - 1 - e^{-(\pi^2 l_x^2)/a^2} \right) - \frac{m\omega^2 l_x^2}{2} - 2\lambda\omega\hbar - \frac{\hbar^2}{2l_x^2 m} \simeq 2V_0 \left(\frac{\pi^2}{4} - 1 \right) . \quad (15)$$

Writing the single particle hopping amplitude as in Eq. (14) remarks the fact that the one-body contributions to the energy are function of the lattice attenuation factor ε as well. In typical experimental situations, the lattice spacing a is usually much larger than the local ground state length l_x at each lattice site. Hence $\varepsilon \ll 1$, and this fact allows to exploit the lattice attenuation factor as a meaningful dimensionless expansion parameter. The first two nontrivial contributions to the one-body part of the energy are proportional to ε , corresponding

to $|i-j| = 1$ and ε^4 , corresponding to $|i-j| = 2$. The first contribution is the usual nearest-neighbor hopping of the standard Bose-Hubbard model, while the second one is a next-to-nearest-neighbor hopping term.

Concerning the two-body contributions to the energy, the classification in powers of ε looks in principle more complicated. However, it is easy to see that all the terms related to pairs of nearest-neighbor sites are proportional to powers ε^l at most of order $l = 2$. On the other hand, energy terms involving pairs of next-to-nearest-neighbors

or triples of three adjacent sites are always smaller, because the leading terms of this two classes of energy contributions are, respectively, proportional to ε^6 and ε^3 . Hence, in the lattice Hamiltonian description of interacting bosonic atoms in periodic optical potentials, we need

$$\hat{H} = \frac{U_0}{2} \sum_i \hat{n}_i (\hat{n}_i - 1) - \frac{J_1}{2} \varepsilon \sum_i (\hat{a}_i^\dagger \hat{a}_{i+1} + H.c.) + U_0 \varepsilon^{\frac{3}{2}} \sum_i [(\hat{a}_i^\dagger \hat{n}_i \hat{a}_{i+1} + \hat{a}_{i-1}^\dagger \hat{n}_i \hat{a}_i) + H.c.] + 2U_0 \varepsilon^2 \sum_i \hat{n}_i \hat{n}_{i+1} + U_0 \varepsilon^2 \sum_i (\hat{A}_i^\dagger \hat{A}_{i+1} + H.c.) , \quad (16)$$

where we have introduced both the on site occupation number operator $\hat{n}_i = \hat{a}_i^\dagger \hat{a}_i$ and the on site pair annihilation operator $\hat{A}_i \equiv \hat{a}_i^2$. The first two terms of Eq. (16) represent the usual BH Hamiltonian with on site interaction and single-atom nearest-neighbor hopping. The remaining terms give the corrections to this model, associated to higher powers of the lattice attenuation factor ε . The term proportional to $\varepsilon^{3/2}$ is the single-boson nearest-neighbor hopping conditioned by the on site occupation; the first term proportional to ε^2 is the density-density nearest-neighbor interaction; and, finally, the second term proportional to ε^2 is the nearest-neighbor hopping of pairs of bosons.

III. THE FREE ENERGY

When dealing with systems of interacting bosons, it is convenient to work in the framework of the grand canonical ensemble [8, 9, 10, 27]. Let us then introduce the grand canonical Hamiltonian \hat{K}

$$\hat{K} = \hat{H} - \mu \sum_i \hat{n}_i , \quad (17)$$

where μ is the chemical potential needed to fix the average total number of bosons in the lattice. All the summations entering in Eq. (17) can be arranged in two different sets (\hat{K}_l) and (\hat{K}_{int}). The first one, (\hat{K}_l), contains all “local” terms that depend only on the on site occupation number operators \hat{n}_i and \hat{n}_{i+1} . The second one, (\hat{K}_{int}) contains all the “non local” hopping terms. According to this grouping, one can write

$$\hat{K} = \hat{K}_l + \hat{K}_{nl} . \quad (18)$$

We will first analyze the EBH model when the second, the third and the last terms of the right-hand side of Eq. (16), i.e. the kinetic contributions to energy, may be neglected and only the local terms are retained (in a sense that will be clarified below).

to consider, in first approximation, only the energy terms proportional to ε^l with $l \leq 2$. At this order of approximation, the lattice Hamiltonian Eq. (9) reads, with the terms ordered in increasing powers of ε ,

A. Local energy terms and mapping to a quantum Ising antiferromagnet

Considering Eq. (16) and Eq. (17), the local energy part in Eq. (18) reads

$$\hat{K}_l = \frac{U_0}{2} \sum_i \hat{n}_i (\hat{n}_i - 1) - \mu \sum_i \hat{n}_i + 2U_0 \varepsilon^2 \sum_i \hat{n}_i \hat{n}_{i+1} . \quad (19)$$

Since in the “local” part of the Hamiltonian we include the nearest-neighbor interaction term, we should qualify that here, by “local” we mean all effects that do not involve particle exchange between sites.

To fix techniques and notations, we first briefly recall how to determine the energy spectrum of the local part of the Hamiltonian in the standard BH model, i.e. when we neglect the term proportional to ε^2 in Eq. (19). In this case, it is well known that each term in the sum of on site interaction energies reaches its minimum for $n_i = n^*$ with

$$n^* = \frac{1}{2} + \frac{\mu}{U_0} . \quad (20)$$

This trivial observation naturally leads to introduce the complete orthonormal Fock basis $\{|n_i\rangle\}$ and determines an obvious but important classification. If n^* is close to an integer value, say n_0 , we have that the energy gap Δ between the ground state $|n_0\rangle$ and the first excited state is of the order of the coupling constant U_0 . This, incidentally, justifies neglecting, in first approximation, any correction proportional to any power $l \geq 2$ of ε . In this situation, at zero temperature, the system is in a Mott-Insulator phase with exactly n_0 atoms per site. On the other hand, if n^* is closer to a half-integer value, then the energy gap Δ can be comparable with other contributions to the interaction energy, and one can write

$$n^* = \frac{1}{2} + n_0 + \frac{2\Delta}{U_0} , \quad (21)$$

where n_0 is integer, $|\Delta|/U_0 \ll 1$ and the two number states nearly degenerate in energy are $|n_0\rangle$ and $|n_0 + 1\rangle$.

This near degeneracy occurs in pairs: the states $|n_0 + 2\rangle$ and $|n_0 - 1\rangle$ (when it exists, i.e. when $n_0 \geq 1$) are as well nearly degenerate and are separated from the pair $\{|n_0\rangle, |n_0 + 1\rangle\}$ by a gap of the order of U_0 . The two nearly-degenerated ground states $|n_0\rangle$ and $|n_0 + 1\rangle$ are separated from each other by an energetic distance equal to $2|\Delta|$, while the gap between the two nearly-degenerate first excited states $|n_0 + 2\rangle$ and $|n_0 - 1\rangle$ is equal to $6|\Delta|$. These results hold analogously for the pairs $\{|n_0 + 3\rangle, |n_0 - 2\rangle\}$ and $\{|n_0 + 4\rangle, |n_0 - 3\rangle\}$, and so on, as long as the second element $|n_0 - k\rangle$ of each pair exists. From this classification, it emerges the fundamental role played by the two nearly degenerate states $|n_0\rangle$ and $|n_0 + 1\rangle$. Moreover, the previous analysis allows to recast the local Hamiltonian Eq. (19) in a very useful form. Introducing the operator $\hat{m}_i \equiv \hat{n}_i - (n_0 + \frac{1}{2})$ and fixing the zero of the energy, the local part of the grand canonical Hamiltonian reads

$$\hat{K}_l = \frac{U_0}{2} \sum_i \left(\hat{m}_i^2 - \frac{1}{4} \right) - 2\delta \sum_i \hat{m}_i + K \sum_i \hat{m}_i \hat{m}_{i+1}, \quad (22)$$

where $\delta \equiv \Delta - 2U_0\epsilon^2(n_0 + \frac{1}{2})$, and $K \equiv 2U_0\epsilon^2$.

The above discussion and Eq. (22) allow a clear understanding of the local part of the EBH model at zero temperature, showing that all the states different from the two quasi degenerate ground states $|n_0\rangle$ and $|n_0 + 1\rangle$ do not contribute. Then, the first term in Eq. (22) can be neglected, and the remaining part of the local Hamiltonian (22) describes an assembly of interacting two-level systems. Actually, because $K > 0$, it is mapped exactly in a spin 1/2 antiferromagnetic quantum Ising model in the presence of an external field -2δ :

$$\hat{H}_{eq} = -2\delta \sum_i \hat{\sigma}_i^z + K \sum_i \hat{\sigma}_i^z \hat{\sigma}_{i+1}^z. \quad (23)$$

At zero temperature, this model describes a system that undergoes a quantum phase transition at the critical field $\delta_c = K/2$. The ferromagnetic phase $|\delta| > \delta_c$ corresponds to the Mott-Insulator phase with the same, constant number of atoms n_0 on each lattice site. The antiferromagnetic phase $|\delta| < \delta_c$ corresponds to a density wave phase with n_0 atoms on a site and $n_0 + 1$ on its neighbor. Analogously to the spin system in the antiferromagnetic phase, the optical lattice for the bosonic atoms in the density wave phase is divided in two sublattices of “staggered” atomic densities n_0 and $n_0 + 1$. In the following, we will denote the two phases, respectively by PMI (Pure Mott-Insulator) and by DWMI (Density Wave Mott-Insulator).

B. Nonlocal energy terms, ferromagnetic- and antiferromagnetic-like models, and the mean field free energy

When the nonlocal hopping terms are reintroduced, the tensor product states of the local occupation number states (local Fock states) are no longer eigenstates of the total Hamiltonian. The true eigenstates cannot be determined analytically, and consistent approximations must be envisaged to approach the problem in the product basis of the local states. Let us first rewrite the nonlocal terms appearing in the grand canonical Hamiltonian (18) in terms of the on site “magnetization” operators \hat{m}_i :

$$\hat{K}_{nl} = -\frac{J}{2} \sum_i \left(\hat{a}_i^\dagger \hat{a}_{i+1} + H.c. \right) + U_0 \epsilon^{\frac{3}{2}} \sum_i \left(\hat{a}_i^\dagger (\hat{m}_i + \hat{m}_{i+1}) \hat{a}_{i+1} + H.c. \right) + \frac{K}{2} \sum_i \left(\hat{A}_i^\dagger \hat{A}_{i+1} + H.c. \right), \quad (24)$$

where the “dressed” hopping amplitude J reads

$$J \equiv \epsilon \left[J_1 - 2U_0 \epsilon^{\frac{1}{2}} \left(n_0 + \frac{1}{2} \right) \right]. \quad (25)$$

From Eq. (25) we see that the density-dependent part of the hopping amplitude gives a negative contribution if the boson-boson interactions are repulsive ($U_0 > 0$). Stability of the ground state energy thus requires

$$J_1 > 2U_0 \epsilon^{\frac{1}{2}} \left(n_0 + \frac{1}{2} \right). \quad (26)$$

Typically, such a stability requirement can be easily satisfied in most experimental situations, unless one goes to

very large occupation numbers n_0 and very strong interaction couplings U_0 . Hence, in the following discussions and examples, we will always consider situations in which the stability condition Eq. (26) is satisfied.

Before introducing mean field approximations, we first need to deal with the second term in Eq. (24), the conditioned hopping term. This can be done, in a Bogoliubov-like framework, by replacing the operator \hat{m}_i with its average value $\chi_i = \langle \hat{m}_i \rangle$, thus neglecting quantum fluctuations. This is justified in the situation in which the magnitude of the on-site interaction amplitude U_0 is sufficiently large that the probability of finding on site occupation numbers that do not fall in the ranges identified by the pairs $\{n_0, n_0 + 1\}$ and $\{n_0 + 2, n_0 - 1\}$ is

negligible. This is the physical situation that one usually meets in realistic experimental conditions. In implementing this approximation we must thus distinguish between two different instances, according to the previous discussion on the local terms.

I - If one has $|\delta| > K/2$, then the approximate model describing the system is ferromagnetic-like and, in the limit of vanishing nonlocal hopping terms, the associated ground state reduces exactly to the PMI phase. In the ferromagnetic-like model, the expectation value of the occupation number χ_i is constant on all sites of the optical lattice: $\chi_i = \chi \forall i$.

II - If one has $|\delta| < K/2$, then the approximate model describing the system is antiferromagnetic-like and, in

the limit of vanishing nonlocal hopping terms, the associated ground state reduces exactly to the DWMI phase. In the antiferromagnetic-like model, the expectation value of the on site occupation number takes opposite values on neighboring sites of the optical lattice: $\chi_i = \chi$, $\chi_{i+1} = -\chi$ and henceforth the conditioned hopping term in Eq. (24) vanishes.

Then, in compact notation, the grand canonical Hamiltonian \hat{K}^F for the ferromagnetic-like case and the grand canonical Hamiltonian \hat{K}^A for the antiferromagnetic-like case read:

$$\hat{K}^{F,A} = \frac{U_0}{2} \sum_i \left(\hat{m}_i^2 - \frac{1}{4} \right) - 2\delta \sum_i \hat{m}_i + K \sum_i \hat{m}_i \hat{m}_{i+1} - \frac{J^{F,A}}{2} \sum_i \left(\hat{a}_i^\dagger \hat{a}_{i+1} + H.c. \right) + \frac{K}{2} \sum_i \left(\hat{A}_i^\dagger \hat{A}_{i+1} + H.c. \right). \quad (27)$$

Here, $J^{F,A}$ are the single particle hopping amplitude of the two models. When $|\delta| > \delta_c$, one must take the choice $J^F = J - 4U_0 \varepsilon^{\frac{3}{2}} \chi$. When $|\delta| < \delta_c$, one must take the choice $J^A = J$.

Before proceeding, we would like to make the following side observation. The grand canonical operator Eq. (27) takes into account both the local and the nonlocal parts of energy. We have seen that when we can neglect the nonlocal terms (i.e. in the absence of the kinetic terms), the local part of the Hamiltonian Eq. (19) is mapped in a spin-1/2 quantum Ising model Eq. (23). We can exploit a similar mapping also for the total Hamiltonian Eq. (27) in the particular limit when the on site interactions are strong enough that the only states that contribute are those with n_0 and $n_0 + 1$ bosons per lattice site. In this special limit, the nearest neighbor atomic pair hopping operator $\hat{A}_i^\dagger \hat{A}_{i+1}$ does not produce any effect. Hence, by the same identifications $\hat{a}_i^\dagger = \hat{\sigma}_i^\dagger = \hat{\sigma}_i^x + i\hat{\sigma}_i^y$ and $\hat{m}_i^\dagger = \hat{\sigma}_i^z$ that map Hamiltonian \hat{K}_l Eq. (19) to the quantum Ising model Eq. (23), the two Hamiltonians $\hat{K}^{F,A}$ Eq. (27) are mapped in the two spin- $\frac{1}{2}$ XXZ Hamiltonians

$$\begin{aligned} \hat{H}_{XXZ}^{F,A} = & -2\delta \sum_i \hat{\sigma}_i^z + K \sum_i \hat{\sigma}_i^z \hat{\sigma}_{i+1}^z \\ & - J^{F,A} \sum_i (\hat{\sigma}_i^x \hat{\sigma}_{i+1}^x + \hat{\sigma}_i^y \hat{\sigma}_{i+1}^y). \end{aligned} \quad (28)$$

The above limiting mapping of Bose-Hubbard models in XXZ Hamiltonians in external field has been investigated extensively by van Otterlo *et al.* [47], who predicted the existence of a supersolid phase in two dimensions.

We are now in a position that allows to introduce mean field approximations on the generic terms contain-

ing pairs of operators an adjacent sites, namely: $\hat{a}_i^\dagger \hat{a}_{i+1}$; $\hat{A}_i^\dagger \hat{A}_{i+1}$; and $\hat{m}_i \hat{m}_{i+1}$. For the latter term, we must make a bookkeeping for the two different model Hamiltonians corresponding to $|\delta| > |\delta_c|$ and $|\delta| < |\delta_c|$. In the first case we must consider $\chi = \langle \hat{m}_i \rangle \forall i$. In the second case the order parameter has opposite signs on adjacent sites. For the first two pairs of terms, in order to implement correctly the mean field approximation, we must make sure that concavity of the energy holds, guaranteeing that the extremal conditions correspond to a true minimum of the energy and not to a maximum. For the single particle hopping, recalling that $-J^{F,A} < 0$ we must consider a uniform order parameter $\langle a_i \rangle = \langle a_i^\dagger \rangle = \phi \forall i$. For the pair hopping term we have that its amplitude K is always positive; hence, in order to obtain the right concavity, we need to choose an order parameter that takes opposite signs on adjacent sites: $\langle A_i \rangle = \psi$, $\langle A_{i+1} \rangle = -\psi$. We have chosen to restrict to real order parameters even if, due to the non-hermiticity of the involved operators, in principle complex order parameters would be allowed. Obviously, the imaginary parts of the order parameters may be easily taken into account. However, we have verified that even in these cases the extremal conditions always lead to real results. For this reason we can restrict our analysis right from the start to real order parameters, a situation that is in complete analogy with the one encountered in the study of the standard on site BH model [9, 10].

We can now write down the mean field expressions for the ferromagnetic-like and antiferromagnetic-like grand canonical total Hamiltonians (with M being the total number of lattice sites):

$$\begin{aligned}
\hat{K}^{F,A} = & \frac{U_0}{2} \sum_i \left(\hat{m}_i^2 - \frac{1}{4} \right) - J^{F,A} \sum_i (\hat{a}_i^\dagger + \hat{a}_i) \phi - (\delta - K\chi) \sum_{i \in S1} \hat{m}_i - (\delta \mp K\chi) \sum_{i \in S2} \hat{m}_i \\
& + \frac{K}{2} \sum_{i \in S1} (\hat{A}_i^\dagger + \hat{A}_i) \psi - \frac{K}{2} \sum_{i \in S2} (\hat{A}_i^\dagger + \hat{A}_i) \psi + (K\psi^2 + J^{F,A}\phi^2 \mp K\chi^2) M,
\end{aligned} \tag{29}$$

where the minus sign holds for the ferromagnetic and the plus sign for the antiferromagnetic case. By $S1$ and $S2$ we denote the two different sublattices in which the original lattice is split with regard to the ψ and χ order parameters (for the latter, only in the case $2|\delta| < K$).

The grand canonical total Hamiltonians are written down as sums of local on site energy terms, and the order parameters $\{\chi, \phi, \psi\}$ must be evaluated self-consistently. In principle, the Fock spaces associated to the on site occupation numbers are infinite-dimensional. However, the leading term in Eq. (29) is the one proportional to U_0 , so that all number states with eigenvalue greater than U_0 can be neglected, leading to consider only the set of

the four lowest lying states that include the two nearly degenerate local states $|n_0\rangle$ and $|n_0+1\rangle$, and the two nearly degenerate local states $|n_0+2\rangle$ and $|n_0-1\rangle$ (when the latter exists, i.e. when $n_0 \geq 1$).

Starting from the two grand canonical Hamiltonians Eq. (29) we can evaluate analytically the two free energies F of the system at any inverse of the temperature $\beta = (k_B T)^{-1}$ either in the ferromagnetic-like or in the antiferromagnetic-like case. One elegant technique to do so is to resort to the resolvent approach, as illustrated in the Appendix. Considering the free energy per site $f^{F,A}$ in the thermodynamic limit, one has:

$$\begin{aligned}
f^{F,A} = & J^{F,A}\phi^2 + K\psi^2 \mp K\chi^2 - \frac{(J^{F,A}\phi)^2(n_0+1) + K^2\psi^2(n_0+1)^2}{U_0} \\
& - \frac{1}{2\beta} \sum_{r=1}^2 \log \left[2 \cosh \left(\beta(\lambda_r + \frac{\alpha_r}{U_0}) \right) \right],
\end{aligned} \tag{30}$$

where

$$\begin{aligned}
\lambda_r = & \sqrt{(\delta - K\chi_r)^2 + (J^{F,A}\phi)^2(n_0+1)}, \\
\alpha_r = & -\frac{1}{\lambda_r} \left\{ 2(J^{F,A}\phi)^2 K \psi_r (n_0+1)^2 + [(J^{F,A}\phi)^2 - K^2 \psi_r^2 (n_0+1)] (\delta - K\chi_r) \right\},
\end{aligned} \tag{31}$$

In Eq. (30) the index r runs over the two sub-lattices $S1$ and $S2$ in which the original lattice is split. In the ferromagnetic case $2|\delta| > K$ the two sublattices coincide and $\lambda_1 = \lambda_2 = \lambda$, $\alpha_1 = \alpha_2 = \alpha$, where

$$\lambda = \sqrt{(\delta - K\chi)^2 + (J^F\phi)^2(n_0+1)} \tag{32}$$

$$\alpha = -\frac{1}{\lambda} \left\{ 2(J^F\phi)^2 K \psi (n_0+1)^2 + [(J^F\phi)^2 - K^2 \psi^2 (n_0+1)] (\delta - K\chi) \right\}. \tag{33}$$

The free energy per site so obtained depends, obviously, on the three order parameters ϕ , ψ and χ , that must be evaluated self-consistently. Regarding ϕ and ψ , this is an easy task; it is accomplished by simply determining the minimum of the free energy in each case. The existence

of the minimum is assured by the right concavity of the free energy and hence it is enough to impose $\partial f / \partial \phi = 0$ and $\partial f / \partial \psi = 0$, in order to determine their extremal values. On the contrary, the order parameter χ , that depends both on ϕ and ψ : $\chi = \chi(\phi, \psi)$, cannot be simply evaluated by fixing the extremality conditions. One must instead resort to its definition, and solve analytically for it, i.e., we must use the fact that χ is defined as the average value of \hat{m}_i and exploit this definition to determine it. This evaluation may be performed using the same mathematical technique employed for the evaluation of the free energy (see the Appendix). The self-consistent equation so obtained together with the extremal condition with respect to the hopping order parameter are the set of relations that are needed to analyze the phase diagram of the

system. As we have already mentioned, the expressions derived for the Hamiltonians and the free energies are obtained and are valid in the moderately strong coupling regime, where only the first four lowest lying states are considered (see the Appendix for more details). This condition is consistently met when the ratio w of the dressed hopping to the on site interaction coupling strength does not exceed unity: $w \equiv J(n_0 + 1)/U_0 < 1$.

IV. RESULTS AND DISCUSSION

The study of the different possible solutions of the three equation needed to determine the different order parameters supplies the information needed about the phase diagram of the system. Obviously, it is not possible to follow analytically all the solutions as functions both of the temperature and of the Hamiltonian parameters, and exact numerical solutions will be used to track the phase diagram in the whole range of physical parameters.

A. Phase diagram: qualitative aspects, absence of pair superfluidity, and the role of many-body interactions

As it is well known, the standard BH model sustains a phase transition between a single-boson superfluid phase and a normal (disordered) phase that at vanishing temperature reduces to a Mott insulator phase [8, 9, 10]. The first issue we wish to address here is whether, due to the presence of energy terms corresponding to the hopping of pairs of atoms between adjacent sites, the EBH model can sustain a new superfluid phase characterized by a non vanishing value of the pair-superfluidity order parameter ψ either in the absence ($\phi = 0$) and/or in the presence ($\phi \neq 0$) of the standard superfluidity of individual atoms. In fact, we find that within the EBH setting this is never the case, and it is always $\psi = 0$. This negative result can be easily understood by looking at the condition of extremality obtained by differentiating Eq. (30) with respect to the pair-superfluidity order parameter for either generic sub-lattice:

$$\psi - \frac{K(n_0 + 1)^2}{U_0} \psi = \frac{1}{2KU_0} \frac{\partial \alpha}{\partial \psi} \tanh \left(\beta \left(\lambda + \frac{\alpha}{U_0} \right) \right), \quad (34)$$

where, for the sake of simplicity, we have omitted the sub-lattice index r . We immediately observe that the left-hand side of Eq. (34) involves both terms proportional to the zero-order power of U_0 and to the inverse of U_0 , while in the right-hand side only the term proportional to the inverse of U_0 appears. Since our analysis is carried out in the strong-coupling limit (large U_0) and the hyperbolic tangent takes values in the range $[-1, 1]$, the extremality condition Eq. (34) is effectively of the form $(1 - A)\psi = B\psi$, with the real coefficients A and

B such that $A \simeq B$. Therefore, it is satisfied only if the pair-superfluidity order parameter ψ vanishes. In fact, one can show that this result holds in general. Taking into account corrections proportional to any power $l > 2$ of ε , they give rise to new hopping terms that are different from the single-particle and pair hoppings that we have considered so far. An example of such hopping terms of higher order is provided by the operator describing the collective tunneling from, say, site i to site j of pairs consisting of two atoms localized on nearest neighbor sites, and so on. Each of these new hopping terms is associated to a suitable order parameter to be determined self-consistently. For these order parameters, the same arguments exploited for ψ hold, implying that the extremality conditions are always and only satisfied if all the order parameters for the superfluidity of composite particles vanish identically. This result leads to a behavior, with respect to superfluidity, that is ruled by the single-atom superfluid order parameter ϕ , and is thus qualitatively similar to that exhibited by the standard BH model at finite temperature, under the effect of a superimposed harmonic confinement [27].

From a fundamental physical point of view, the impossibility to obtain a superfluid phase in which the tunneling particles are composite bosons made up by two or more bosonic atoms stems from the fact that the local eigenstates of lowest on-site energy are always the two consecutive Fock states $|n0\rangle$ and $|n_0 + 1\rangle$. This always makes the hopping of any aggregate of atoms energetically unfavorable. To engineer a superfluid phase of composite bosons is thus necessary to overcome this limitation and realize a situation in which the two lowest local eigenstates of lowest on site energy are $|n0\rangle$ and $|n_0 + k\rangle$, with $k > 1$ being the dimensionality of the generic composite. To achieve this goal is then necessary to engineer and take into account many-body interactions comparable in magnitude to the standard bilinear ones (two-body collisions) that are usually the only interactions included in the description of dilute systems of interacting bosons.

In the following, we will first consider the ferromagnetic model to track the SF-PMI quantum phase transition as the zero-temperature limit of the the finite-temperature transition between the disordered and the superfluid phase. Later on, we will consider the anti-ferromagnetic model to determine the SF-DWMI phase transition, and, finally, we will analyze the full quantum phase diagram of the EBH model at zero temperature.

B. Finite- and zero-temperature transitions to superfluidity

Starting from the “ferromagnetic” grand canonical free energy, the critical diagram for single atom superfluidity is reported in Fig. 1 for different sets of values of the Hamiltonian parameters. From Fig. 1, we observe a lowering of the critical temperature T_c^F with increasing amplitude of the energy gap Δ . From a physical point view,

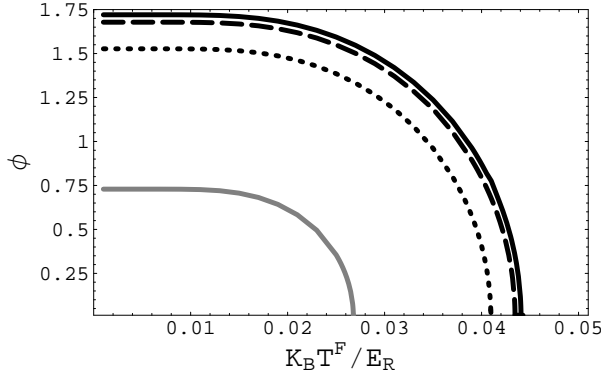


FIG. 1: Single atom superfluid order parameter ϕ , as a function of the dimensionless “ferromagnetic” critical temperature $k_B T^F / E_R$ rescaled in units of the lattice recoil energy E_R , for $J = 0.01U_0$. From top to bottom, behavior for $\Delta = 0$ (black solid line), $\Delta = 0.009U_0$ (dashed line), $\Delta = 0.02U_0$ (dotted line), and $\Delta = 0.04U_0$ (solid line). Notice, as expected, that the critical temperature lowers as the energy gap Δ increases.

this situation is due to the fact that for high values of Δ , bosons experience a high potential barrier that contrasts the hopping from a site to its nearest neighbor with a consequently increasing difficulty for the whole system to go toward an ordered phase and hence the superfluid transition occurs in “colder” zones. Solving the equation $\partial f / \partial \phi|_{\psi=0} = 0$ with χ evaluated at $\psi = \phi = 0$, we get

$$\beta_c^F = \frac{1}{\delta - H\chi(0,0)} \tanh^{-1} \left[\frac{2/(J - H\chi(0,0)) - 2(n_0 + 1)/U_0}{(n_0 + 1)/(\delta - K\chi(0,0)) - 2/U_0} \right], \quad (35)$$

where $H = 2U_0\varepsilon^{\frac{3}{2}}$. In Fig. 2 we show the behavior of the critical temperature in units of the lattice recoil energy E_R as a function of the filling factor $n = n_0 + 1/2 + \chi$ for different values of the Hamiltonian parameters. Due to the existence of a region with density wave order, the condition $\chi = 0$ or $n = n_0 + 1/2$ is verified throughout an entire (although small) region in the space of parameters rather than at a given point in it. In this region the critical temperature, as we will see in the following, becomes function of the DWMI order parameter χ , while the filling factor remains constant. Hence Fig. 2 reproduces the behavior of the critical temperature only in the ferromagnetic-like instance, and the value of the critical temperature with semi-integer value of the filling factor requires a longer analysis that will be presented in the following subsection. Fig. 2 shows the competition between thermal effects and ordered mobility. At fixed n , a larger hopping amplitude corresponds to a higher critical temperature. In Fig. 3 we show instead the behavior of the critical temperature as a function of the optical lattice depth $s \equiv V_0/E_R$ for different values of the chemical potential. As the depth of the lattice increases, hopping and mobility are suppressed, and the critical temperature of the superfluid transition lowers.

Looking back at Fig. 2 we must notice that, obviously, the critical temperature vanishes for integer value of the filling factor (no superfluidity allowed). Requiring instead that β_c^F assumes an infinite value in Eq. (35), we obtain the critical condition on the local gap or “exter-

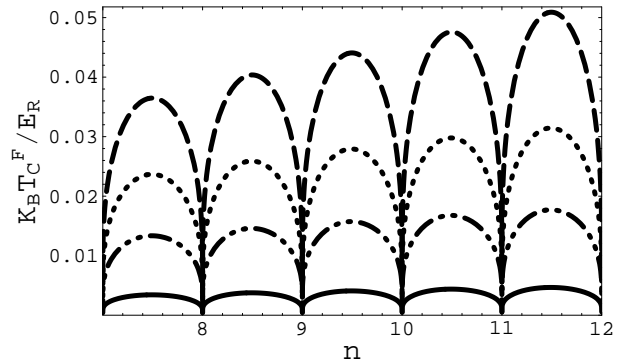


FIG. 2: Dimensionless critical temperature $k_B T_c^F / E_R$, rescaled in units of the lattice recoil energy E_R , for the transition between the disordered (high-temperature) phase and the superfluid (low-temperature) phase as a function of the filling factor n . From top to bottom, functional behavior for $J = 0.01U_0$ (dashed line), $J = 0.007U_0$ (dotted line), $J = 0.004U_0$ (dashed-dotted line), and $J = 0.001U_0$ (solid line). As the overall hopping J increases, the critical temperature rises.

nal magnetic field” δ for the zero-temperature quantum phase transition from a PMI phase to superfluidity:

$$\delta_c^F = \frac{(J - H/2)(n_0 + 1)}{2 \left(1 - \frac{n_0(J - H/2)}{U_0} \right)} + \frac{K}{2}. \quad (36)$$

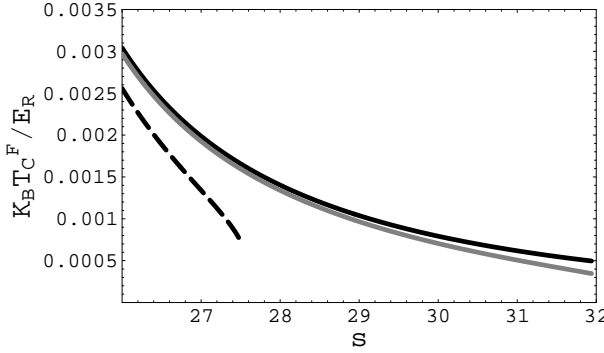


FIG. 3: Dimensionless critical temperature $k_B T_c^F / E_R$, rescaled in units of the lattice recoil energy E_R , for the transition to superfluidity as a function of the dimensionless lattice depth $s \equiv V_0 / E_R$. From top to bottom, behavior for $\Delta = 0$ (solid black line), $\Delta = 0.0005 U_0$ (solid gray line), and $\Delta = 0.0009 U_0$ (dashed black line).

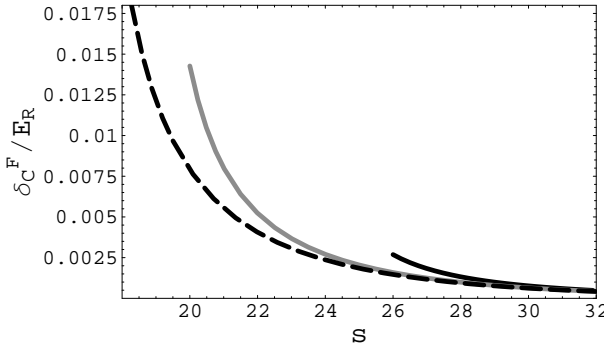


FIG. 4: Dimensionless critical field δ_c^F / E_R , as a function of the lattice depth s . From left to right, behavior for $\lambda = 65$ (dashed black line), $\lambda = 39$ (solid gray line), $\lambda = 13$ (solid black line).

If the local “gap” δ is smaller than δ_c^F , the system is in a superfluid phase; otherwise, a Mott insulator is realized. Clearly, this result holds provided that $\delta > \frac{K}{2}$, i.e the system cannot access the density wave region. The behavior of δ_c^F as function of the depth of the optical lattice

is showed in Fig. 4, for different values of the anisotropy parameter occurring in the external harmonic confinement. Concerning Fig. 3, we observe that the functional behavior is not plotted down to small values of the lattice depth parameter s . This is due to the fact that for values of s in the approximate range $[0, 15]$, the weak coupling ratio $w = J(n_0 + 1)/U_0$ may exceed unity, so that the strong coupling approximation breaks down. The graph has thus been plotted in the interval of values of s such that $0 \leq w \leq 0.6$. We observe that the critical temperature decreases for increasing s . This is due to the fact that the greater the lattice depth, the more the on-site interaction tends to dominate on the hopping. Hence, in order to achieve the onset of the transition to the ordered superfluid phase it is necessary to operate at lower temperatures. Moreover, once the lattice depth is fixed, the critical temperature is lower for larger energy gap Δ , in agreement with the results presented in Fig. 1. Concerning Fig. 4, each of the three curves, corresponding to a different value of the transverse trapping frequency (anisotropy parameter), is plotted for a different range of the lattice depth s . Each of these different ranges corresponds to the different zones in which, for the various values of the anisotropy parameter, the relation $0 \leq w \leq 0.6$ holds. We see that the range of permissible values of s grows with increasing anisotropy.

C. Unified finite-temperature phase diagram

The transition from an ordered superfluid phase to a Density Wave Mott Insulator can be determined starting from the antiferromagnetic grand canonical free energy along the same lines followed to analyze the SF-PMI phase transition in the ferromagnetic grand canonical setting. Hence, we will analyze the zero-temperature SF-DWMI quantum phase transition by first determining the “antiferromagnetic” critical temperature T_c^A and critical field, δ_c^A , the associated finite-temperature phase diagram, and by finally taking the zero-temperature limit. Concerning the first step, straightforward evaluation yields:

$$1 - \frac{J(n_0 + 1)}{U_0} = J \sum_{r=1}^2 \left\{ \tanh [\beta_c^A (\delta + K\chi_r(0, 0))] \left(\frac{n_0 + 1}{\delta + K\chi_r(0, 0)} - \frac{2(\delta + K\chi_r(0, 0))}{U_0 \sqrt{(\delta + K\chi_r(0, 0))^2}} \right) \right\}, \quad (37)$$

for the inverse β_c^A of the “antiferromagnetic” critical temperature, and

$$\delta_c^A = \frac{J U_0 (n_0 + 1) + \sqrt{4K^2(J(1+n_0) - U_0)^2 + (J U_0 (n_0 + 1))^2}}{4(U_0 - J(1+n_0))} \quad (38)$$

for the “antiferromagnetic” critical field, that differs analytically from the “ferromagnetic” one expressed by Eq. (36). Of course, in those regions of the space of parameters that allow to neglect the nonlocal energy terms, δ_c^A and δ_c^F coincide exactly. The relations expressed by Eq. (37) and Eq. (38) together with the corresponding ones previously obtained for the SF-PMI phase transition allow us to construct the full phase diagram of the EBH model both at finite and at zero temperature.

Concerning the finite-temperature scenario, we report in Fig. 5 the behavior of the critical temperature for the transition from the high-temperature disordered phase to the low-temperature ordered superfluid phase as a function of the energy gap Δ for different values of the lattice parameters. Recalling the relation $\delta \equiv \Delta - 2U_0\epsilon^2(n_0 + \frac{1}{2})$ that connects the local external field with the energy gap, we can follow the entire evolution of the critical temperature as a function of the external field, moving smoothly through the ferromagnetic and the antiferromagnetic regimes. The thermodynamic evolution of the system may be considered made up of three continuous intervals. Going from left to right on the abscissa in Fig. 5, the interval of negative values of Δ , that maps in the interval of negative values $\delta < -K/2$, corresponds to a ferromagnetic critical temperature $T_c = T_c^F$. The central part of the interval, around $\Delta = 0$, corresponds to the interval of negative and positive values $-K/2 < \delta < K/2$ and to an antiferromagnetic critical temperature $T_c = T_c^A$. Finally, the right part of the interval of positive values of Δ that maps in the interval of positive values $\delta > K/2$, corresponds again to a ferromagnetic critical temperature $T_c = T_c^F$.

In the central interval, the finite-temperature analogue of the zero-temperature SF-DWMI quantum phase transition is realized (antiferromagnetic-like coupling). In the two external regions the finite-temperature analogue of the zero-temperature SF-PMI quantum phase transition is realized (ferromagnetic-like coupling). In the former, antiferromagnetic-like case, the behavior of the critical temperature as the gap varies in the range $[-K/2, K/2]$ should be represented by a flat, constant line in the central region of Fig. 5, joining the two curves representing the critical temperature in the two ferromagnetic-like external regions. However, due to its extremely small extension, this “antiferromagnetic connection” appears shrunk to a single point, the overall maximum of the critical temperature. Hence, the only visible landscape in the regions above the critical temperature in Fig. 5 is the one relative to the finite-temperature analogue of the zero-temperature arrangements in which a Pure Mott Insulator arrangement is favored. In these regions, the

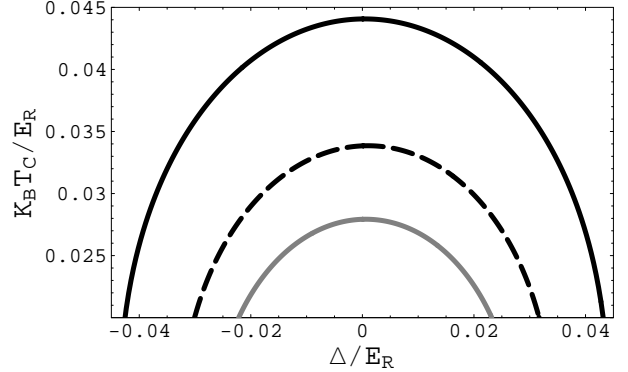


FIG. 5: The critical temperature $k_B T_c / E_R$ for the transition from a disordered phase to the ordered superfluid phase as a function of the local energy gap Δ / E_R . From top to bottom, behavior for $J = 0.01 U_0$ (black solid line), $J = 0.009 U_0$ (dotted line), and $J = 0.007 U_0$ (gray solid line).

critical temperature lowers as the modulus of the gap increases. This fact is in agreement with the considerations developed for Fig. 1. In particular, when the modulus of the gap is larger than the value of the critical field for the SF-PMI quantum phase transition, the critical temperature vanishes and the lattice is characterized by the same, constant integer filling factor on all sites. Moreover, by using the same arguments presented in the previous subsection for the behavior of the critical temperature as a function of the filling factor, we can understand the lowering of the critical temperature as a consequence of the lowering of the hopping amplitude from a site to its nearest neighbor.

D. Unified zero-temperature quantum phase diagram: Superfluid, Pure Mott Insulator, and Density Wave Mott Insulator phases

To conclude our study, we can now consider the full diagram of quantum phases at zero temperature, by taking the limit $\beta_c \rightarrow 0$. At zero temperature, the quantities that determine the transition from a kind of ordering to another one are the Hamiltonian parameters, that are controllable quantities. When the ratios of these control parameters are suitably tuned, macroscopic changes take place in the ground state of the system. These changes give rise to the zero temperature phase diagram that we report in Fig. 6. Here the control parameters are the magnitude of the nearest neighbor hopping amplitude J and the local energy gap δ . In establishing the boundaries between the different phases, we must take into account

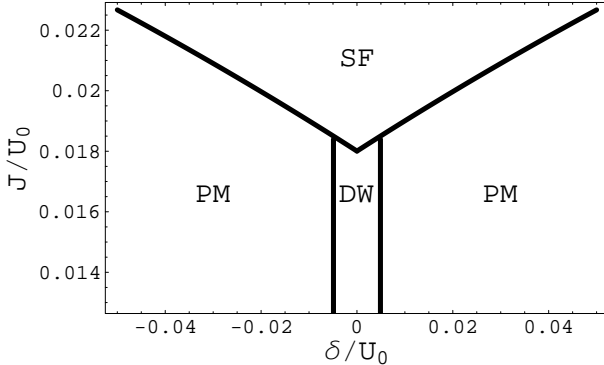


FIG. 6: The zero-temperature quantum phase diagram of the EBH model in the strong coupling regime. Horizontal axis: dimensionless gap δ/U_0 . Vertical axis: dimensionless normalized hopping amplitude J/U_0 . The vertical lines are the separation lines between the DWMI and PMI phases. The oblique lines are the separation lines between the SF and PMI phases and between the SF and DWMI phases. Symmetrically placed on the sides of the cusp point are the two tricritical points. The phase diagram is plotted for a value of the lattice attenuation factor $\varepsilon = 0.07$ and on site occupation $n_0 = 9$. Here the label PM stands for Pure Mott, DW for Density Wave, and SF for SuperFluid.

that δ_c^F and δ_c^A essentially coincide in a wide range of values of the lattice parameters. These two quantities determine, respectively, the boundary lines at the quantum phase transitions from the SF to the PMI phase, and from the SF to the DWMI phase. The quantity δ_c instead determines the boundary line at the quantum phase transition from the DWMI to the PMI ordering. An important novelty emerges with respect to the phase diagram of the standard BH model. In fact, in this last case there exists only one boundary line, the one separating the SF from the PMI phase. However, in the quantum phase diagram of the EBH model, two further boundary lines appear.

The first one is the coexistence curve for the SF and the DWMI orderings; the second one is the coexistence curve for the two insulating phases, the PMI and the DWMI. The three different boundary lines cross at two triple points where all the three phases coexist. From Fig. 6 and Fig. 7, describing the zero-temperature phase diagram for two different values of the lattice attenuation factor ε , we of course see that the zone in which the system is in a DWMI phase is extremely small compared to the regions occupied by the SF and PMI phases. This could be already expected from the shrinking to a point of the corresponding antiferromagnetic-like plateau in the finite-temperature diagram reported in Fig. 5.

Comparison of the two phase diagrams reported in Fig. 6 and Fig. 7 shows that the lattice attenuation factor plays a crucial role concerning the area in the space of parameters in which the system is in a DWMI phase. The smaller is the value of ε the smaller and less observable becomes the region in which the DWMI phase takes

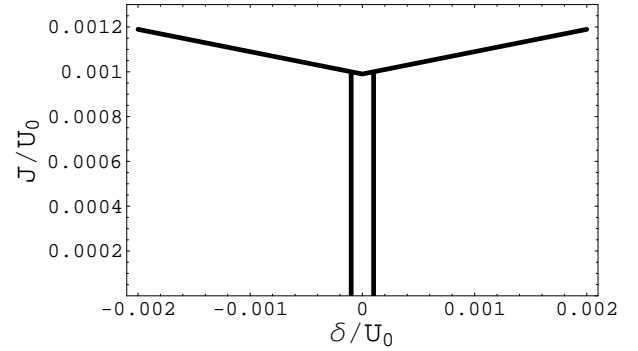


FIG. 7: The zero-temperature quantum phase diagram of the EBH model in the strong-coupling regime, plotted for $\varepsilon = 0.01$ and $n_0 = 9$. Labels denoting the various quantum phases have been omitted, as the meaning of the oblique and vertical lines is the same as in Fig. 6. Notice, in particular, the dramatic shrinking of the density wave phase for a lower value of ε , compared to the one fixed in Fig. 6.

place. This fact implies that the experimental observation of such a phase will require significant advances in the manipulation and control of systems of interacting bosons in optical lattice potentials. In particular, it will be important to combine optical lattices potentials and magnetic Feshbach resonances to enhance the on site interactions to strong coupling limits, while at the same time keeping the lattice attenuation factor in a range of not too exceedingly small values.

V. CONCLUSIONS AND OUTLOOK

We have studied systems of ultracold spin-zero neutral bosonic atoms with repulsive interactions, harmonically trapped and regularly arranged by means of a periodic optical lattice potential. Taking into account the series expansion of the amplitudes of the interaction terms in powers of the lattice potential parameters and of the lattice attenuation factor, we have mapped the second-quantized total Hamiltonian in a new, specific form of Extended Bose Hubbard (EBH) Hamiltonian. We have then established various mappings of this atomic EBH model to models of interacting spin- $\frac{1}{2}$ systems. By using such a correspondence, we have analyzed in a unified way the Density Wave and Pure Mott Insulator phases supported by the model, in analogy with the unified mean field treatment of ferro- and anti-ferromagnetism.

We have developed the mean field theory description of the EBH model both at finite and zero temperature, determining the free energy density, and analyzing the finite-temperature behavior of the model, determining the phase boundaries between the ordered superfluid and the disordered high-temperature phase. We have demonstrated the theoretical possibility for two different transitions to superfluidity within the EBH model, one due

to the hopping of single atoms, and the other due to the hopping of atomic pairs. In fact, we have given a thermodynamical proof that only the first mechanism is realized if one truncates the expansion in the lattice attenuation parameter at lowest order. Finally, we have determined the zero temperature phase diagram of the EBH model, showing the existence of a new quantum phase, the Density Wave Mott Insulator, which is not allowed within the framework of the standard BH model, and we have determined the range of lattice and Hamiltonian parameters for which such a phase can be detected. The two different forms of localized phases, Pure Mott Insulator and Density Wave Mott Insulator, manifest themselves, respectively, in the different behavior of the atomic density in the lattice. The PMI phase is characterized, as usual, by the same, constant integer filling factor throughout the entire lattice; the DWMI is instead characterized by two different integer filling factors in two sublattices, say n_0 for half of the lattice sites, and $n_0 + 1$ on their neighbors (checkerboard phase). We have studied the behavior of typical physical quantities of the system, illustrating how the different control parameters involved compete in determining the evolution of the system.

Regarding future perspectives, it is to be expected that by taking the expansion of the second-quantized total Hamiltonian further up to higher powers in the lattice attenuation factor, a new, and accordingly very small region in the phase diagram will emerge where pair superfluidity, absent both in the BH and in the EBH model, can occur, at least at extremely high filling factors, as well as new types of intermediate range interactions and tunneling mechanisms. The same framework introduced in this paper may be extended to the case of systems of interacting bosons when the excited harmonic levels of the trapping potential [27] and/or the higher-excited Bloch bands of the optical lattice potential [43, 44] are taken into account. It would be an interesting challenge to further extend the scheme developed in the present work for pure single-flavor bosons with repulsive interactions to the case of multi-flavor bosons and/or attractive interactions; to mixtures of bosonic and fermionic atoms interacting on a lattice [16, 48, 49]; and, finally, to the case of disordered and/or random optical lattices that allow for the study of disordered ultracold atomic gases [50, 51].

APPENDIX

In this appendix, we will briefly review the resolvent method [52] needed to obtain the expression Eq. (30) for the free energy of the EBH model.

In order to study the thermodynamic properties of the system in the grand canonical ensemble, we must determine the corresponding partition function, Z :

$$Z = \text{Tr}[\exp(-\beta \hat{K}^{F,A})], \quad (\text{A.1})$$

where $\hat{K}^{F,A}$ is given by Eq. (29) and $\beta = 1/k_B T$ with

k_B the Boltzmann constant. By writing down the explicit form of $\hat{K}^{F,A}$, the grand canonical partition function reads

$$Z = \text{Tr}\left\{\exp\left[-\beta\sum_i(\hat{h}_i + J^{F,A}\phi^2 + K\psi^2 \mp K\chi^2)\right]\right\}. \quad (\text{A.2})$$

In the last equation \hat{h}_i represents the action of the operator

$$\hat{h} \equiv \sum_i \hat{h}_i = \sum_i (\hat{h}_L + \hat{h}_I) \quad (\text{A.3})$$

on the i -th lattice site. As we may deduce from Eq. (29), the first operator appearing inside the sum in the right-hand side of Eq. (A.3) is the Hamiltonian whose eigenstates are tensor products of local Fock states $|n_0 + k\rangle$ with k integer or zero:

$$\sum_i \hat{h}_L = \frac{U_0}{2} \sum_i \left(\hat{m}_i^2 - \frac{1}{4} \right) - \delta \left(\sum_{i \in S1} \hat{m}_i + \sum_{i \in S2} \hat{m}_i \right), \quad (\text{A.4})$$

while the second operator is the mean-field “decoupled version” of operators representative of the single-boson hopping, atomic-pair hopping, and of the density-density interaction $\hat{m}_i \hat{m}_j$, respectively:

$$\begin{aligned} \sum_i \hat{h}_I = & -J^{F,A} \sum_i (\hat{a}_i^+ + \hat{a}_i) \phi \\ & + K\chi \sum_{i \in S1} \hat{m}_i - (\mp K\chi) \sum_{i \in S2} \hat{m}_i \\ & + \frac{K}{2} \sum_{i \in S1} (\hat{A}_i^+ + \hat{A}_i) \psi \\ & - \frac{K}{2} \sum_{i \in S2} (\hat{A}_i^+ + \hat{A}_i) \psi. \end{aligned} \quad (\text{A.5})$$

In Eq. (A.4) and Eq. (A.5), the indexes $S1$ and $S2$ denotes the two sub-lattices in which the whole lattice is split. The meaning of the parameters $J^{F,A}$ and K have been already explained in Sections II and III.

From the grand canonical partition function, the expression for the free energy $F^{F,A} = -\frac{1}{\beta} \ln Z$ of the system is readily deduced. This thermodynamic potential will depend, in general, on the mean field parameters of the theory.

We describe our system in the complete basis of the number states. Keeping in mind that we are analyzing the physics of our system in the mean field approximation, correlations between different lattice sites are neglected and hence, the partition function Z of the systems factorizes into the product of M independent partition functions, each of these evaluated for a single site. In the Fock states basis and in mean field approximation framework, the grand canonical partition function then reads

$$Z = \left[\sum_{n=0}^{\infty} \langle n | \exp(-\beta(\hat{h}_i + J^{F,A}\phi^2 + K\psi^2 \mp K\chi^2)) | n \rangle \right]^M$$

$$\mp K\chi^2))|n>\Big]^M, \quad (\text{A.6})$$

where M is the total number lattice sites, the sum is in principle performed over all Fock states, and it is intended that the thermodynamic limit must be eventually taken. However, as already discussed in Section III, for sufficiently strong coupling we may limit ourselves to consider the four Fock states of lowest energy $|n_0>$, $|n_0+1>$, $|n_0-1>$, and $|n_0+2>$ (actually, in the ultra-strong coupling regime, it is enough to consider only the

two lowest states [47]). This choice is fully justified as long as the weak coupling parameter $w \equiv J(n_0 + 1)/U_0$ does not approach or exceed unity. In this way we can determine the expressions of the physical quantities of interest in the EBH model at first order in powers of $1/U_0$. To evaluate the free energy, one needs to compute the trace of the operator $\exp(-\beta\hat{h}_i)$. However, rather than diagonalizing \hat{h}_i in the space spanned by the four lowest-lying Fock states, it is more convenient to write the free energy per site $f^{F,A}$ in the following way:

$$\begin{aligned} f^{F,A} \equiv \frac{F^{F,A}}{M} &= J^{F,A}\phi^2 + K\psi^2 \mp K\chi^2 - \frac{1}{2\beta} \sum_{r=1,2} \left(\ln \left(\sum_{j=-1}^2 \langle n_0 + j | \exp(-\beta\hat{h}_i) | n_0 + j \rangle \right) \right)_r \\ &= J^{F,A}\phi^2 + K\psi^2 \mp K\chi^2 - \frac{1}{2\beta} \sum_{r=1,2} \left(\ln \left(\sum_{j=-1}^2 I_j \right) \right)_r, \end{aligned} \quad (\text{A.7})$$

where

$$I_j = \frac{1}{2\pi i} \oint dz \exp(-\beta z) G_{j,j}(z), \quad (\text{A.8})$$

and for any couple of integers or zeroes (j, k) ,

$$G_{j,k}(z) = \langle n_0 + j | (z - \hat{h}_i)^{-1} | n_0 + k \rangle \quad (\text{A.9})$$

is the Green function connecting the eigenstates $|n_0 + j>$ and $|n_0 + k>$ of \hat{h}_L . The index r appearing in Eq. (A.7) is the sub-lattice index. The operator $(z - \hat{h}_i)^{-1}$ appearing in the right-hand side of Eq. (A.9) is the so-called “resolvent operator”. To evaluate the Green functions

$G_{j,k}(z)$, we have to know how the resolvent operator acts on the ket $|n_0 + k>$. According to Eq. (A.3), the action of the Hamiltonian operator \hat{h}_i is nothing but the action of the operator \hat{h}_L plus the action of the operator \hat{h}_I . Their action can be determined explicitly as follows. If \hat{A} and \hat{B} are two operators, the following identity holds:

$$\frac{1}{\hat{A}} - \frac{1}{\hat{B}} = \frac{1}{\hat{A}}(\hat{B} - \hat{A})\frac{1}{\hat{B}} = \frac{1}{\hat{B}}(\hat{B} - \hat{A})\frac{1}{\hat{A}}. \quad (\text{A.10})$$

Then, with the identifications $\hat{A} = z - \hat{h}_i$ and $\hat{B} = z - \hat{h}_L$, one has

$$\frac{1}{z - \hat{h}_i} = \frac{1}{z - \hat{h}_L} + \frac{1}{z - \hat{h}_i} \hat{h}_I \frac{1}{z - \hat{h}_L} = \frac{1}{z - \hat{h}_L} + \frac{1}{z - \hat{h}_L} \hat{h}_I \frac{1}{z - \hat{h}_i}. \quad (\text{A.11})$$

The right-hand side of Eq. (A.11) will be useful in the evaluation of the propagators $G_{j,k}(z)$ in the basis formed by the eigenstates of \hat{h}_L . In principle, for each values of j , one needs to construct a $p \times p$ system of equations in the variables $G_{j,k}(z)$, where the order p of each system is equal to the cardinality of the chosen basis. On the other hand, only those functions $G_{j,k}(z)$ connecting basis vectors will give non-vanishing contributions. Hence,

in our case we have to deal with four systems, each of these made up of four equations. We will write down the explicit form of such a system for the variables $G_{j,j}(z)$ that, as we can see from the Eq. (A.7), are the needed quantities to determine the free energy per site. In each sub-lattice labeled by r , and omitting the index for the function $G_{j,j}(z)$, we have

$$\delta_{j,0} = (z + (\delta - K\chi_r)) G_{0,0}(z) + \frac{J^{F,A} \sqrt{n_0 + 1}}{2} G_{1,1}(z) \phi + \frac{J^{F,A} \sqrt{n_0}}{2} G_{-1,-1}(z) \phi$$

$$\begin{aligned}
& -\frac{K\sqrt{(n_0+1)(n_0+2)}}{2}G_{2,2}(z)\psi_r; \\
\delta_{j,1} &= (z - (\delta - K\chi_r))G_{1,1}(z) + \frac{J^{F,A}\sqrt{n_0+1}}{2}G_{0,0}(z)\phi \\
& + \frac{J^{F,A}\sqrt{n_0+2}}{2}G_{2,2}(z)\phi - \frac{K\sqrt{n_0(n_0+1)}}{2}G_{-1,-1}(z)\psi_r; \\
\delta_{j,-1} &= (z - U_0 + 3(\delta - K\chi_r))G_{-1,-1}(z) \\
& + \frac{J^{F,A}\sqrt{n_0}}{2}G_{0,0}(z)\phi - \frac{K\sqrt{n_0(n_0+1)}}{2}G_{1,1}(z)\psi_r; \\
\delta_{j,2} &= (z - U_0 - 3(\delta - K\chi_r))G_{2,2}(z) + \frac{J^{F,A}\sqrt{n_0+2}}{2}G_{1,1}(z)\phi \\
& - \frac{K\sqrt{(n_0+1)(n_0+2)}}{2}G_{0,0}(z)\psi_r
\end{aligned} \tag{A.12}$$

Therefore, when $j = 0$, $j = 1$, $j = -1$, and $j = 2$ solving system Eq. (A.12) provides, respectively, $G_{0,0}(z)$, $G_{1,1}(z)$, $G_{-1,-1}(z)$, and $G_{2,2}(z)$ in each sub-lattice. Each of these solutions may be written as

$$G_{j,j}(z) = \frac{N_j(z)}{D(z)}. \tag{A.13}$$

Since we are operating in the strong-coupling regime, we retain only the contributions proportional to non-vanishing powers of U_0 in $N_j(z)$ and $D(z)$. We can now obtain the explicit expression for the free energy by direct evaluation of the second line of Eq. (A.7). First, the integrals I_j appearing in Eq. (A.8) are solved by the usual integration techniques in the complex plane, and we determine the poles of the functions $G_{j,j}(z)$ by solving the equation

$$D(z) = 0. \tag{A.14}$$

The roots of Eq. (A.14) provide the eigenvalues of the Hamiltonian \hat{h}_i at the needed order of approximation and allows to calculate explicitly the right-hand side of Eq. (A.8). Finally, inserting the expressions for the quantities I_j in the second line of Eq. (A.7), yields the desired expression for the free energy per site Eq. (30).

The method of the resolvent allows as well to obtain the explicit expression for the mean field order parameter χ in each sub-lattice. Following the same procedure adopted to evaluate the free energy per site, the “mean number” χ in a given sub-lattice can be determined by the formula

$$\begin{aligned}
\chi &= \frac{1}{2} \left[\frac{\sum_n \langle n | \hat{n} \exp(-\beta \hat{h}_i) | n \rangle}{\sum_n \langle n | \exp(-\beta \hat{h}_i) | n \rangle} - (n_0 + \frac{1}{2}) \right] \\
&= \frac{1}{2} \left[\frac{n_0 I_0 + (n_0 + 1) I_1 + (n_0 - 1) I_{-1} + (n_0 + 2) I_2}{I_0 + I_1 + I_{-1} + I_2} - (n_0 + \frac{1}{2}) \right],
\end{aligned} \tag{A.15}$$

where the integer index n runs over the finite number of local eigenstates being considered. The magnetization of

the generic sub-lattice r finally reads

$$\chi_r = \frac{1}{2} \left\{ -\frac{\delta - K\chi_r}{2\lambda_r} \tanh \left[\beta \left(\lambda_r + \frac{\alpha_r}{U_0} \right) \right] - \frac{(J^{F,A}\phi)^2(n_0+1)}{2U_0\lambda_r^3} \left[\left(2K(n_0+1)(\delta - K\chi_r)\phi^2\psi + K^2\psi^2(n_0+1) \right. \right. \right. \\$$

$$-(J^{F,A}\phi)^2\right)\tanh\left[\beta\left(\lambda_r+\frac{\alpha_r}{U_0}\right)\right]\right\}, \quad (\text{A.16})$$

where

$$\begin{aligned} \lambda_r &= \sqrt{(\delta - K\chi_r)^2 + (J^{F,A}\phi)^2(n_0 + 1)}, \\ \alpha_r &= -\frac{1}{\lambda_r} \left[2(J^{F,A}\phi)^2 K \psi_r (n_0 + 1)^2 + ((J^{F,A}\phi)^2 - K^2 \psi_r^2 (n_0 + 1))(\delta - K\chi_r) \right]. \end{aligned} \quad (\text{A.17})$$

In the ferromagnetic-like case, the single atom hopping amplitude is J^F , so that $\chi_1 = \chi_2 = \chi$, and the two sub-lattices are characterized by the same magnetization, that is, by the same constant filling factor n_0 . In the antiferromagnetic-like case, the single atom hopping

amplitude is J^A , so that $\chi_1 = -\chi_2 = \chi$, and the two sub-lattices have opposite magnetizations, that is, two different constant filling factors n_0 and $n_0 + 1$, respectively.

[1] M. Greiner, I. Bloch, O. Mandel, T. W. Hänsch, and T. Esslinger, Phys. Rev. Lett. **87**, 160405 (2001).
[2] C. Orzel, A. K. Tuchman, M. L. Fenslau, M. Yasuda, and M. A. Kasevich, Science **291**, 2386 (2001).
[3] M. Greiner, O. Mandel, T. Esslinger, T. W. Hänsch and I. Bloch, Nature **415**, 39 (2002).
[4] M. Greiner, O. Mandel, T. Esslinger, T. W. Hänsch and I. Bloch, Nature **419**, 51 (2002).
[5] J.R. Anglin and W. Ketterle, Nature **416**, 211 (2002).
[6] P. S. Jessen and I. H. Deutsch, Adv. At. Mol. Opt. Phys. **37**, 95 (2002).
[7] S. Sachdev, *Quantum Phase Transitions* (Cambridge University Press, Cambridge, 1999).
[8] M. P. A. Fisher, P. B. Weichman, G. Grinstein, and D. S. Fisher, Phys. Rev. B **40**, 546 (1989).
[9] D. van Oosten, P. van der Straten, and H. T. C. Stoof, Phys. Rev. A **63**, 053601 (2001); Phys. Rev. A **67**, 033606 (2003).
[10] K. Sheshadri, H. R. Krishnamurthy, R. Pandit, and T. V. Ramakrishnan, Europhys. Lett. **22**, 257 (1993).
[11] J. Ruostekoski, G. V. Dunne, and J. Javanainen, Phys. Rev. Lett. **88**, 180401 (2002).
[12] W. Hofstetter, J. I. Cirac, P. Zoller, E. Demler, and M. D. Lukin, Phys. Rev. Lett. **89**, 220407 (2002).
[13] B. Paredes and J. I. Cirac, Phys. Rev. Lett. **90**, 150402 (2003).
[14] A. Recati, P. O. Fedichev, W. Zwerger, and P. Zoller, Phys. Rev. Lett. **90**, 020401 (2003).
[15] H. P. Büchler, G. Blatter, and W. Zwerger, Phys. Rev. Lett. **90**, 130401 (2003).
[16] F. Illuminati and A. Albus, Phys. Rev. Lett. **93**, 090406 (2004).
[17] A. J. Kerman, V. Vuletic, C. Chin, and S. Chu, Phys. Rev. Lett. **84**, 439 (2000).
[18] P. S. Jessen, D. L. Haycock, G. Klose, G. A. Smith, I. H. Deutsch, and G. K. Brennen, Quant. Inf. and Comput. **1**, 20 (2001).
[19] L. M. Duan, E. Demler, and M. D. Lukin, Phys. Rev. Lett. **91**, 090402 (2003).
[20] I. H. Deutsch, G. K. Brennen, and P. S. Jessen, Fortschr. Phys. **48**, 925 (2000).
[21] D. Jaksch, H. J. Briegel, J. I. Cirac, C. W. Gardiner, and P. Zoller, Phys. Rev. Lett. **82**, 1975 (1999).
[22] J. J. Garcia-Ripoll and J. I. Cirac, Phys. Rev. Lett. **90**, 127902 (2003).
[23] U. Dorner, P. Fedichev, D. Jaksch, M. Lewenstein, and P. Zoller, Phys. Rev. Lett. **91**, 073601 (2003).
[24] J. K. Pachos and P. L. Knight, Phys. Rev. Lett. **91**, 107902 (2003).
[25] D. Jaksch, C. Bruder, J. I. Cirac, C. W. Gardiner, and P. Zoller, Phys. Rev. Lett. **81**, 3108 (1998).
[26] W. Zwerger, J. Opt. B: Quantum Semiclass. Opt. **5**, S9 (2003).
[27] S. M. Giampaolo, F. Illuminati, G. Mazzarella, and S. De Siena, Phys. Rev. A **70**, 061601(R) (2004).
[28] R. Roth and K. Burnett, Phys. Rev. A **68**, 023604 (2003).
[29] P. Buonsante, V. Penna, and A. Vezzani, Phys. Rev. A **70**, 061603(R) (2004).
[30] P. Buonsante, V. Penna, and A. Vezzani, Phys. Rev. A **72**, 031602(R) (2005).
[31] P. Buonsante, R. Burioni, D. Cassi, and A. Vezzani, Phys. Rev. B **66**, 094207 (2002).
[32] P. Buonsante, R. Burioni, D. Cassi, V. Penna, and A. Vezzani, Phys. Rev. B **70**, 224510 (2004).
[33] K. B. Efetov, and A. I. Larkin, Zh. Eksp. Teor. Fiz. **69**, 75 1975 [Sov. Phys. JETP **42**, 390 (1976)].

- [34] V. J. Emery, Phys. Rev. B **14**, 2989 (1976).
- [35] V. J. Emery, in *Chemistry and Physics of One-Dimensional Metals*, edited by H. J. Keller (Plenum, New York, 1977).
- [36] S. Robaszkiewicz, R. Micnas, and K. A. Chao, Phys. Rev. B **23**, 1447 (1981).
- [37] S. Robaszkiewicz, R. Micnas, and K. A. Chao, Phys. Rev. B **24**, 1579 (1981).
- [38] V. J. Emery, in *Highly Conducting One-Dimensional Solids*, edited by J. T. Devreese (Plenum, New York, 1979).
- [39] J. Solyom, Adv. Phys. **28**, 201 (1979).
- [40] H. Q. Lin, E. Gagliano, D. K. Campbell, E. H. Fradkin, and J. E. Gubernatis, in *The Hubbard Model: Its Physics and Mathematical Physics*, edited by D. Baeriswyl, D. K. Campbell, J. M. P. Carmelo, F. Guinea, and E. Louis (Plenum, New York, 1995); H. Q. Lin, D. K. Campbell, and R. T. Clay, Chin. J. Phys. **38**, 1 (2000).
- [41] H. Heiselberg, cond-mat/0510688.
- [42] F. Massel and V. Penna, cond-mat/0506316.
- [43] V. W. Scarola and S. Das Sarma, cond-mat/0503378, Phys. Rev. Lett. **95**, 033003 (2005).
- [44] A. Isacsson and S. M. Girvin, cond-mat/0506622.
- [45] E. Vives, T. Castan, and A. Planes, Am. J. Phys. **65**, 907 (1997).
- [46] G. Modugno, F. Ferlaino, R. Heidemann, G. Roati, and M. Inguscio, Phys. Rev. A **68**, 011601(R) (2003).
- [47] A. van Otterlo, K. H. Wagenblast, R. Baltin, C. Bruder, R. Fazio, and G. Schön, Phys. Rev. B **52**, 16176 (1995).
- [48] A. Albus, F. Illuminati, and J. Eisert, Phys. Rev. A **68**, 023606 (2003); M. Cramer, J. Eisert, and F. Illuminati, Phys. Rev. Lett. **93**, 190405 (2004).
- [49] M. Lewenstein, L. Santos, M. A. Baranov, and H. Fehrmann, Phys. Rev. Lett. **92**, 050401 (2004); R. Roth and K. Burnett, Phys. Rev. A **69**, 021601(R) (2004); L. D. Carr and M. J. Holland, cond-mat/0501156.
- [50] A. Sanpera, A. Kantian, L. Sanchez-Palencia, J. Zajzewski, and M. Lewenstein, Phys. Rev. Lett. **93**, 040401 (2004).
- [51] A. D. Sen, U. Sen, M. Lewenstein, V. Ahufinger, M. Pons, A. Sanpera, quant-ph/0508018; V. Ahufinger, L. Sanchez-Palencia, A. Kantian, A. Sanpera, and M. Lewenstein, cond-mat/0508042
- [52] F. de Pasquale, G. L. Giorgi, and S. Paganelli, Phys. Rev. A **71**, 042304 (2005).